

Yb³⁺, Tm³⁺ and Ho³⁺ triply-doped tellurite core-cladding optical fiber for white light generation

D. Manzani,^{1,*} Y. Ledemi,^{1,3} I. Skripachev,^{1,3} Y. Messaddeq,^{1,3} S. J. L. Ribeiro,¹
R. E. P. de Oliveira,² and C. J. S. de Matos,²

¹Laboratory of Photonics Materials, Institute of Chemistry, UNESP, Araraquara, SP, Brazil

²Grupo de Fotônica, Universidade Presbiteriana Mackenzie, São Paulo/SP, Brazil

³Present address: Center of Optic, Photonic and Laser, University of Laval, Québec, Canada
**danilo.manzani@gmail.com*

Abstract: Tellurite glass is proposed as a host for Yb³⁺, Tm³⁺ and Ho³⁺ triply doped optical fiber and, in this work, a new multimode optical fiber with triply-doped core was fabricated. We report results on the processing and characterization of tellurite-based glass preforms and fibers. Cr³⁺ was used as tracer to assess core quality and uniformity across 60 mm length preform. By Raman fluorescence of Tm³⁺ ions contained into the core, we also mapped the interface between core and cladding that reveals an interface around 45 μm for a 10.11 mm of preform. For triply-doped core fiber excited at 980 nm, we generated white light radiation. The chromaticity diagram showed the multicolor emission and the color tunability of the triply-doped core optical fiber.

©2011 Optical Society of America

OCIS codes: (060.2290) Fiber materials; (060.2310) Fiber optics; (160.2540) Fluorescent and luminescent materials; (160.4670) Optical materials; (160.5690) Rare-earth-doped materials.

References and links

1. G. E. Rachkovskaya and G. B. Zakharevich, "IR spectra of tellurium germanate glasses and their structure," *J. Appl. Spectrosc.* **74**(1), 86–89 (2007).
2. E. R. Taylor, L. N. Ng, N. P. Sessions, and H. Buerger, "Spectroscopy of Tm³⁺-doped tellurite glasses for 1470 nm fiber amplifier," *J. Appl. Phys.* **92**(1), 112–117 (2002).
3. L. F. Johnson and H. J. Guggenheim, "Infrared-pumped visible laser," *Appl. Phys. Lett.* **19**(2), 44–47 (1971).
4. F. E. Auzel, "Materials and devices using double-pumped-phosphors with energy transfer," *Proc. IEEE* **61**(6), 758–786 (1973).
5. E. Downing, L. Hesselink, J. Ralston, and R. Macfarlane, "A three-color, solid-state, three-dimensional display," *Science* **273**(5279), 1185–1189 (1996).
6. T. Honda, T. Doumuki, A. Akella, L. Galambos, and L. Hesselink, "One-color one-beam pumping of Er³⁺-doped ZBLAN glasses for a three-dimensional two-step excitation display," *Opt. Lett.* **23**(14), 1108–1110 (1998).
7. G. S. Maciel, A. Biswas, R. Kapoor, and P. N. Prasad, "Blue cooperative upconversion in Yb-doped multicomponent sol-gel processed silica glass for three-dimensional display," *Appl. Phys. Lett.* **76**(15), 1978–1980 (2000).
8. S. Xu, H. Ma, D. Fang, Z. Zhang, and Z. Jiang, "Tm³⁺/Er³⁺/Yb³⁺-codoped oxyhalides tellurite glasses as materials for three-dimensional display," *Mater. Lett.* **59**(24-25), 3066–3068 (2005).
9. H. T. Amorin, M. V. D. Vermelho, A. S. Gouveia-Neto, F. C. Cassanjes, S. J. L. Ribeiro, and Y. Messaddeq, "Red-green-blue upconversion emission and energy-transfer between Tm³⁺ and Er³⁺ ions in tellurite glasses excited at 1.064 μm," *J. Solid State Chem.* **171**(1-2), 278–281 (2003).
10. Z. Yang and Z. Jiang, "Frequency upconversion emissions in layered lead-germanate-tellurite glasses for three-color display," *J. Non-Cryst. Solids* **351**(30-32), 2576–2580 (2005).
11. J. Canning, M. Stevenson, T. K. Yip, S. K. Lim, and C. Martelli, "White light sources based on multiple precision selective micro-filling of structured optical waveguides," *Opt. Express* **16**(20), 15700–15708 (2008).
12. A. Mori, Y. Ohishi, M. Yamada, H. Ono, and S. Sudo, in *Optical Fiber Communication Conference*, Vol. 2 of 1997 OSA Technical Digest Series, Washington, D.C. (Optical Society of America, 1997), paper PDP1.
13. J. Wang, S. Prasad, K. Kiang, R. K. Pattnaik, J. Toulouse, and H. Jain, "Source of optical loss in tellurite glass fibers," *J. Non-Cryst. Solids* **352**(6-7), 510–513 (2006).
14. A. Jha, P. Joshi, S. Shen, and L. Huang, "Spectroscopic characterization of signal gain and pump ESA in short-lengths of RE-doped tellurite fibers," *J. Non-Cryst. Solids* **353**(13-15), 1407–1413 (2007).
15. J. G. Titchmarsh, "Double crucible method of optical fiber manufacture," U.S. patent no. 4.217.123 (1978).

16. N. Prasad, J. Wang, R. Pattnaik, H. Jain, and J. Toulouse, "Preform fabrication and drawing of KNbO₃ modified tellurite glass fiber," *J. Non-Cryst. Solids* **352**(6-7), 519–523 (2006).
17. D. C. Tran, C. F. Fisher, and G. H. Sigel, "Fluoride glass preforms prepared by a rotational casting process," *Electron. Lett.* **18**(15), 657–658 (1982).
18. V. V. Sakharov, P. B. Baskov, O. V. Akimova, V. Sh. Berikashvili, and G. F. Lebedev, "Fluoride glasses for multifunctional multifiber systems," *Inorg. Mater.* **44**(12), 1386–1392 (2008).
19. Y. Ledemi, D. Manzani, S. J. L. Ribeiro, and Y. Messaddeq, "Multicolor up conversion emission and color tunability in Yb³⁺/Tm³⁺/Ho³⁺ triply doped heavy metal oxide glasses," *Opt. Mater.* **33**(12), 1916–1920 (2011).
20. J. Massera, A. Haldeman, D. Milanese, H. Gebavi, M. Ferraris, P. Foy, W. Hawkins, J. Ballato, R. Stolen, and L. Petit, "Processing and characterization of core-clad tellurite glass preforms and fibers fabricated by rotational casting," *Opt. Mater.* **32**(5), 582–588 (2010).
21. N. Q. Wang, X. Zhao, C. M. Li, E. Y. B. Pun, and H. Lin, "Upconversion and color tunability in Tm³⁺/Ho³⁺/Yb³⁺ doped low phonon energy bismuth tellurite glasses," *J. Lumin.* **130**(6), 1044–1047 (2010).
22. D. L. Yang, H. Gong, E. Y. B. Pun, X. Zhao, and H. Lin, "Rare-earth ions doped heavy metal germanium tellurite glasses for fiber lighting in minimally invasive surgery," *Opt. Express* **18**(18), 18997–19008 (2010).

1. Introduction

Glasses containing heavy oxides such as TeO₂, GeO₂, Bi₂O₃ and PbO are promising materials for near infrared (IR) technologies, non-linear optics and design of new laser devices [1]. Tellurite glasses have been intensively investigated because of their structural and optical properties, including low phonon energy (~750 cm⁻¹) [2], extended infrared transmittance (from 0.4 μm to about 6 μm), high non-linear and linear refractive indices and high rare earth ions (RE) solubility. Moreover, these glasses also exhibit good mechanical, thermal and rheological properties which enable optical fiber production. Their ability to incorporate high concentrations of RE ions also makes them suitable candidates for the development of many kinds of active photonic devices. Infrared to visible up-conversion has been extensively studied since the past decade in RE-ion doped glasses for their potential applications towards solid-state lasers, optical information processing, displays and other photonic devices [3]. For applications in illumination and color displays, it is necessary to generate and control the intensities of the primary red (R), green (G) and blue (B) emissions [4]. Downing et al. have generated the three primary colors from heavy metal fluoride glasses doped with RE ions using three different pairs of near-infrared excitation sources [5]. Later, efficient one color emissions such as green emission from Er³⁺-doped fluoride glass [6] or blue emission from Yb³⁺-doped silicate glass [7] have been reported. More recently, great attention has been paid to generating white light from solid-state materials by controlling the intensities of each RGB emissions [8,9]. Er³⁺, Tm³⁺ and Yb³⁺ ions were used but it has been difficult to simulate the white light due to the quenching of up-converted emission [10]. Also, white light generation has been obtained in a photonic crystal fiber that is triply filled with dye solutions [11].

The choice of suitable host glass matrix for the rare earth ion dopants is a key factor. In the optical amplification process, the pumping efficiency and the emission bandwidth strongly depend on the structural properties of the host glass. The demonstration of a broadband Er³⁺-doped tellurite fiber amplifier in 1997 [12] has led to an extensive research activity using tellurite-based glasses for a range of optical applications [13]. Recently, Jha et al. measured a maximum relative amplification gain, in 50-100 mm tellurite-based optical fibers in the C- (1535 nm) and L- (1560 nm) bands, of 30 dB and 15 dB, respectively [14].

In this paper, we present a method of fabrication used to prepare core-cladding fiber preform structures, called the "sucking method", for tellurite-based glasses. Firstly, we describe the method and results that show the uniformity of the cladding and core layer thicknesses and the quality of their interface, which is supported by Micro Raman spectroscopy. After validating this method and defining the appropriate fabrication conditions, tellurite-based core-cladding glass preforms whose core is triply doped with Tm³⁺, Yb³⁺ and Ho³⁺ ions have been prepared. Multicolor (RGB) visible up conversion emission was investigated by exciting a fiber drawn from such a preform with a 980 nm diode laser. The utilization of the fabricated optically active core-cladding tellurite optical fibers is discussed therein.

2. Experimental setup

Among the different techniques already reported for preparing heavy-oxide glass preforms for core-cladding optical fiber drawing, the main ones are: (i) the double crucible method [15], (ii) the rod in tube technique [16] and (iii) the rotational casting process, developed by Tran et al. in 1982 to develop fluoride-based fibers [17]. In this work, we describe a different method to obtain tellurite core-cladding preforms that allow fabrication of preforms longer than 50-100 mm in length and around 10 mm in diameter with good core-cladding interface quality and core circularity [18].

2.1. Core-cladding preform preparation and optical fiber drawing

Both core and cladding glass compositions were prepared by the conventional melt-casting method. The starting powdered materials were tellurium dioxide TeO_2 (3N), germanium oxide GeO_2 (5N), bismuth oxide Bi_2O_3 (3N) and potassium carbonate K_2CO_3 (3N); the rare earth ions have been incorporated into the core glass by using ytterbium oxide Yb_2O_3 (3N), thulium oxide Tm_2O_3 (3N) and holmium oxide Ho_2O_3 (5N). For a better readability, the host glass is labelled TGBK. In the first step, the powders of both core and cladding compositions were weighed in order to obtain a 12.5g core glass and a 40.0g cladding glass whose molar composition were $70\text{TeO}_2\text{-}15\text{GeO}_2\text{-}10\text{Bi}_2\text{O}_3\text{-}5\text{K}_2\text{O}:(1.6\text{Yb}^{3+}/0.6\text{Tm}^{3+}/0.1\text{Ho}^{3+})$ and $70\text{TeO}_2\text{-}15\text{GeO}_2\text{-}10\text{Bi}_2\text{O}_3\text{-}5\text{K}_2\text{O}$, respectively. It is well known that the core glass should exhibit a linear refractive index slightly higher than that of the cladding glass in order to satisfy the waveguide equations for guided modes within the core. The presence of RE ions into the core glass is responsible for the core refractive index increase. The dopants concentrations were determined according to our previous study [19] and we used 1.6/0.6/0.1% in mass, respectively. After mixing the precursor powders, the batches were melted in a pure gold crucible at 760°C during 2 hours in a conventional furnace, ensuring the complete elimination of CO_2 from the decomposition of the carbonate and good homogenization and fining.

The next step consisted of casting the melts into a special cylindrical stainless steel mould, with 10.11 mm of internal diameter, which was preheated at a temperature close to the glass transition temperature. This cylindrical mould was equipped with a piston whose movement along the cylinder revolution axis (downward) was electrically controlled. This step, which is the most critical of this method, can be described according to three subsequent parts, as presented in Fig. 1: (A) the 40.0g melt batch for the cladding composition is cooled down in a conical section of the preheated mould, and immediately the central piston is driven downward at a constant speed. As the piston descends, the cladding melt is sucked into the cylindrical section of the mould, following the piston motion. The melt solidifies in contact with the mould inner wall, which itself favors the "suction" effect. When a tube is formed with the cladding melt, part (B) starts with the core batch melt being poured over the previous one. This time, the descent of the piston causes the suction of the core composition into the cladding glass tube, thus forming a core-cladding structure, part (C). The piston motion is stopped when the cast of the core begins to form a tube within the mould. Finally, the core-cladding preform is annealed at the same temperature for 12 h and is then slowly cooled down to room temperature in order to minimize residual internal stress.

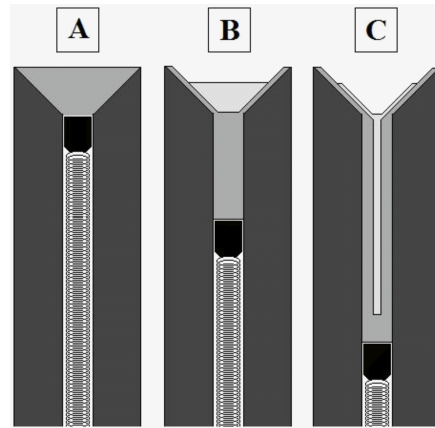


Fig. 1. “Sucking method” experimental setup to prepare core-cladding preforms: cladding glass casting (A), core glass casting during the piston descent (downward) (B) and end of the process (C).

Since the quality and light-guiding efficiency of a fiber is directly dependent on the quality of the preform, it is crucial that the latter presents (i) well controlled core and cladding dimensions, (ii) a highly uniform index step, Δn , between core and cladding throughout the preform and (iii) minimum levels and quantity of defects within both core and cladding glasses. Defects such as cracks and bubbles can cause light scattering that reduces the guiding efficiency of the fiber, inducing large losses and also degrading the mechanical integrity of the fiber. These problems, which largely depend on the glass viscosity as a function of temperature, can be monitored by adjusting the glass composition [20]. The following special care procedures were taken during the preform preparation in order to minimize the formation of defects which would, otherwise, be present afterwards in the fiber: (i) long melting time with constant stirring at a temperature slightly below that of TeO_2 vaporization in step one of the process to ensure the complete elimination of CO_2 from the decomposition of the carbonate and to allow good homogenization and fining; (ii) increasing of the batch viscosity before casting; and (iii) adequate subsequent annealing followed by a slow cooling down to room temperature to minimize residual internal stress and avoid the formation of micro cracks.

In order to check the reproducibility and to determine the adequate parameters of the “*sucking method*” for the production of core-cladding preforms based on the TGBK glass system, previous preparations have been achieved from the same glass composition, but doping the core with 1mol% of Cr_2O_3 instead of the RE ions. The color-center formation property of chromium ions Cr^{3+} (tracer ion) was utilized here to measure and monitor the core diameter versus the cladding diameter, the core centricity and also the core-cladding interface uniformity along the preform length (height). This quality monitoring was accomplished by slicing the preform into cross-sections which were optically polished and visually inspected using a PENTAX digital camera. Around 15 slices with a thickness of ~ 3 mm were extracted from the preform, which had an outer diameter of 10.11 mm. Thus, the adequate parameters to obtain a core-cladding preform with the desired geometry and reproducibility have been determined and afterwards used to prepare preforms with RE ion doped core. Finally, the interface uniformity of the latter was controlled by taking advantage of the presence of Tm^{3+} ions into the core. Indeed, that ion exhibits an intense emission band centred at 800 nm when excited at 633 nm, corresponding to the radiative relaxation $^3\text{H}_4 \rightarrow ^3\text{H}_6$, and such transition can be readily monitored by using a HORIBA Jobin Yvon model LabRAM HR micro Raman apparatus equipped with a 632.8 nm excitation laser with 30 mW power. In addition, the quality of the triply doped core-cladding preform interface was investigated by mapping the region using the Tm^{3+} fluorescence band centered at 3210 cm^{-1} (~ 800 nm).

The step-index optical fiber was then drawn by pulling the preform using an optical fiber drawing tower at the Institute of Chemistry, UNESP, Brazil. The drawing temperature for this composition was found to be 380°C. The optical fiber had an outer (cladding) diameter of ~125 μm when drawn at a speed of 7 m/min. In this case, the core diameter was around 30 μm . Around 300 m of fiber were obtained from 50 mm of preform. Note that all fibers were drawn without polymer coating; their mechanical strength was, indeed, good enough to be handled throughout all the characterization measurements reported here. Nonetheless, our facilities allow us to cover the fiber with a protective polymeric coating for a further use. In order to ensure that the drawing conditions did not induce neither nucleation nor crystallization, the temperature of the tower furnace (hot zone and pre-heat zone) was mapped and the time in this zone was controlled before and during the drawing process.

2.2. Triply doped core optical fiber characterization

Firstly, undoped core optical fibers were prepared for background loss measurement and waveguide characterization. Optical losses of 9.8dB/m were measured at 632.8 nm, using the cut-back method in a 700 mm fiber length. It must be said that such loss includes intrinsic fiber loss and rare-earth ions absorption. From the measured refractive index profile, the numerical aperture (NA) of this fiber can be calculated to be 0.1849.

Then, optical fibers with triply doped core were drawn for white light generation. Luminescence was obtained with a 145 mW laser diode at 980 nm as the pump source, which was pigtailed to a single mode fiber. The pump was coupled into a 100-400 mm length of the triply doped fiber via butt coupling. Light at the fiber output traversed a 320-720 nm bandpass filter before being detected in a spectrometer. The power in each emission band was obtained from the total power (measured in a powermeter) multiplied by the fraction of the spectrum corresponding to the given band.

In addition, near-field images of the emission exiting the fiber were obtained with an objective lens and a digital camera containing a CMOS detector. The white light emission was also filtered using red, green and blue bandpass filters to separate the three RGB emissions. All measurements have been performed at room temperature.

3. Results and discussion

3.1. Preform preparation and characterization

As mentioned in the previous section, to probe the uniformity of the core diameter along the preform, a Cr_2O_3 doped preform was sliced, as shown in the outset of Fig. 2. The individual slice measurements were plotted in Fig. 2, which illustrates the variation of core-cladding preform dimensions over the 60 mm length. Curve B (black) corresponds to the cladding diameter measurements while curve A (red) corresponds to the core diameter measurements. The core diameter ranged from 5.15 to 4.20 mm and the cladding diameter remained constant at 10.11 mm. Between preform lengths of 16 and 51 mm (X axis in the figure), the core had a diameter of 4.20 mm with good center uniformity along the 35 mm of preform length. Moreover, the undoped glass (cladding) remained colorless compared with the Cr^{3+} -doped glass (core), showing minimal apparent diffusion of Cr^{3+} from the doped glass to the undoped glass during the core-cladding preform processing.

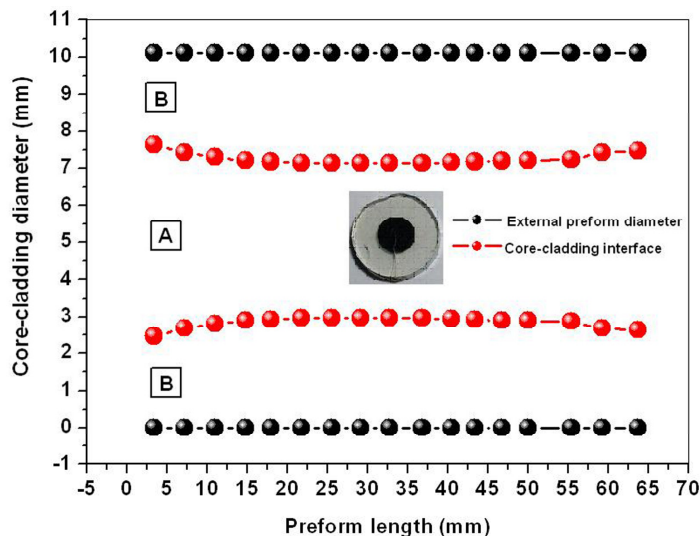


Fig. 2. Evolution of the core and cladding diameters over the length of the preform prepared using the sucking method, measured at multiple cross-section locations.

As mentioned above, the key point which requires special attention in the preform production is the quality of the core-cladding interface. To characterize more precisely the interface quality for the triply-doped core preform (density gradient), as well as any diffusion of the RE ions to the cladding, this region was scanned by Micro Raman spectroscopy, while monitoring the emission intensity of the Tm^{3+} ion when excited at 632.8 nm. Figure 3 shows the Raman spectra for the core and cladding regions of the preform. In the latter, it can be clearly observed two main enveloped bands centered at 450 and 750 cm^{-1} , indicating Te-O-Te and TeO bonding stretches from the glass host, respectively. Between 2400 and 4000 cm^{-1} , one can observe the characteristic Raman bands of the Tm^{3+} and Ho^{3+} ions contained in the core glass composition. In the Fig. 3, band 1 (2550 cm^{-1}) corresponds to the Ho^{3+} transition $^5\text{S}_2, ^5\text{F}_4 \rightarrow ^5\text{I}_7$ and both bands 2 and 3 (3215 and 3345 cm^{-1}) are assigned to the Tm^{3+} transition $^3\text{H}_4 \rightarrow ^3\text{H}_6$ (inset of Fig. 3). The strongest emission, at $\sim 3210 \text{ cm}^{-1}$ ($\sim 800\text{nm}$), was used to monitor the interface region.

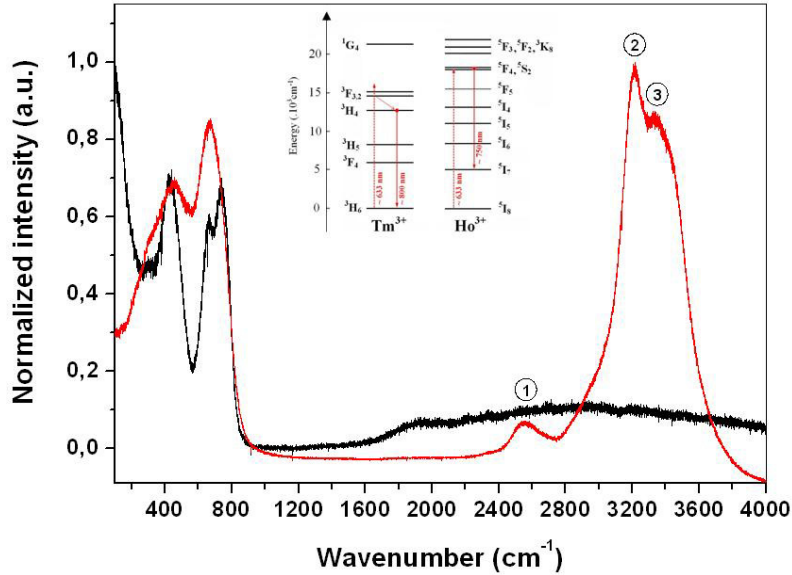


Fig. 3. Raman spectra for the core (red line) and cladding (black line) regions. The inset is the simplified Tm^{3+} ions energy diagram with the involved electronic transitions upon 632.8 nm excitation.

Figure 4 shows the intensity of emission band 2 as a function of the radial position of the preform. The position scan starts at $-300 \mu\text{m}$, with zero position located almost at the interface, and stops at $+300 \mu\text{m}$ (X axis), as illustrated in the figure inset. Forty Raman spectra have been collected from perform radial surface (focused with microscope aid) to plot the intensity of the 3210 cm^{-1} band. In the -300 to $-60 \mu\text{m}$ range, no emission band was observed in the Raman spectra, confirming the absence of Tm^{3+} ion diffusion into the cladding beyond $60 \mu\text{m}$ from the interface (lateral resolution of $\pm 1 \mu\text{m}$). The $800\text{nm } \text{Tm}^{3+}$ emission band appears at $x = -60 \mu\text{m}$, and its intensity sharply increases from $-50 \mu\text{m}$ to reach a maximum value near $0 \mu\text{m}$. This maximum value then remains approximately constant along the scanned core region, as expected. This plotting technique has allowed us to estimate accurately an interface range of about $45 \mu\text{m}$ for a preform of 10.11 mm in diameter and with $\sim 4.14 \text{ mm}$ of core diameter.

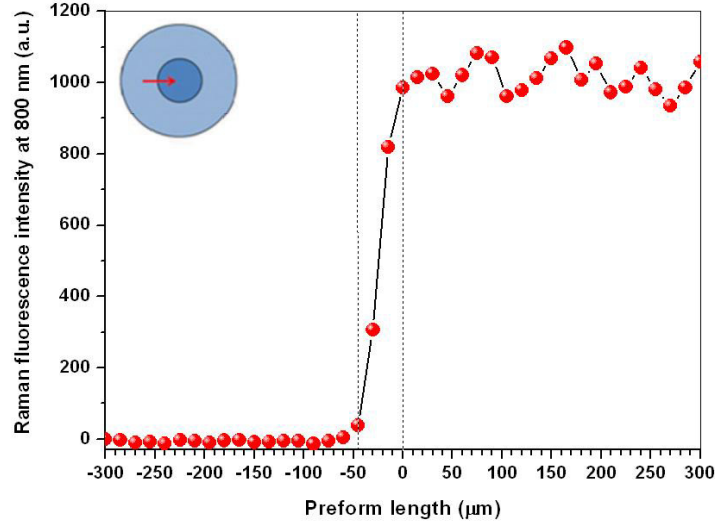


Fig. 4. Raman fluorescence intensity of the band centered at 800 nm under excitation at 632.8 nm as a function of the radial distance on the preform, measured for decreasing radii as indicated by the arrow in the inset.

From both of the two characterizations implemented here (Cr^{3+} core doped and Raman fluorescence), the obtained preforms showed satisfactory quality allowing the fabrication of core-clad preforms with desired index.

3.2. Multicolor up conversion emission in the RE ion triply-doped optical fiber

Figure 5 shows the transmission spectrum obtained when a 500-1700 nm supercontinuum source was launched into 150 mm of the triply-doped fiber. A broad absorption is visible at 950 nm, as well as narrower absorption bands centered at 800, 690, 640 and 540 nm. These absorption bands correspond to the excitations of the rare-earth ions from their ground state, and can be attributed to the following transitions: (i) at 950 nm: $^2F_{7/2} \rightarrow ^2F_{5/2}$ of Yb^{3+} ions; (ii) at 800, 640 and 540 nm: $^5I_8 \rightarrow ^5I_4$, $^5I_8 \rightarrow ^5F_3$ and $^5I_8 \rightarrow ^5F_4, ^5S_2$ of Ho^{3+} ions, respectively; and (iii) at 800 and 690 nm: $^3H_6 \rightarrow ^3H_4$ and $^3H_6 \rightarrow ^3F_2, ^3F_3$ of Tm^{3+} ions, respectively. The absorption band expected at around 450 nm ($^5I_8 \rightarrow ^5G_6$ of Ho^{3+} ion) could not be detected due to the limited source band.

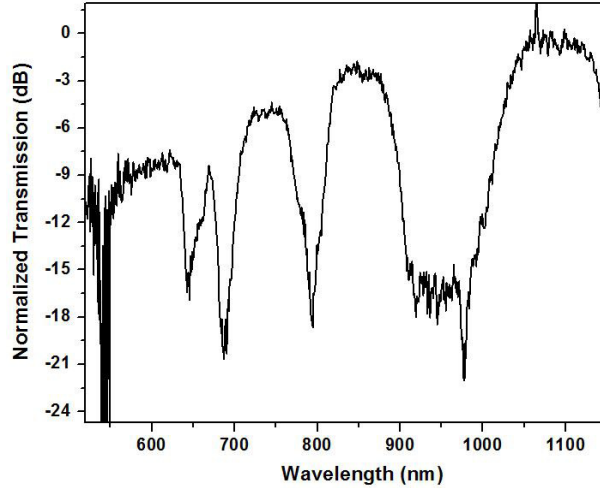


Fig. 5. Normalized transmission spectrum obtained in a 150 mm long fiber with a supercontinuum source.

A 250 mm length of the optical fiber with the triply-doped core was then characterized for up conversion emission with the setup previously described in section 2.2. Figure 6 presents the up conversion spectra collected at the end of the optical fiber, pumped at 980 nm, with a cw laser power ranging from 48 to 145 mW. We can observe the three emission bands centered at 655, 545 and 480 nm, corresponding to red, green and blue colors, respectively. The intense and broad red up-converted emissions (650 and 660 nm) correspond to two contributions: (i) the $^5F_5 \rightarrow ^5I_8$ transition of the Ho^{3+} ions and (ii) the $^1G_4 \rightarrow ^3F_4$ transition of the Tm^{3+} ions. On the other hand the blue up-converted emission (480 nm) originates from the $^1G_4 \rightarrow ^3H_6$ transition of the Tm^{3+} ions; whereas the green up-converted signal (545 nm) originates from the $^5F_4, ^5S_2 \rightarrow ^5I_8$ transition of the Ho^{3+} ions.

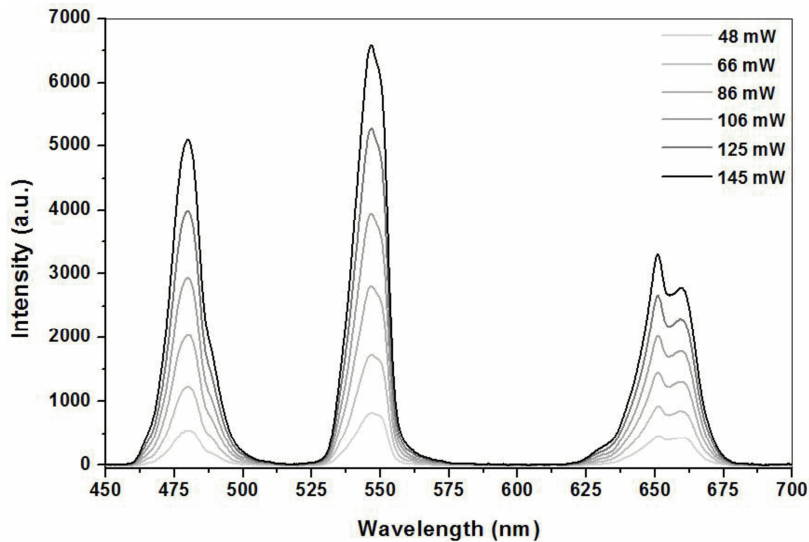


Fig. 6. Up conversion emission spectra of the Yb^{3+} , Tm^{3+} , Ho^{3+} triply-doped core fiber, pumped with a diode laser at 980 nm under 48 to 145mW range of power.

The fiber length was then optimized for maximum output emission power, with a 150 mm length found to be optimum. Figure 7 shows the output power in each emission band, as well

as the total emission power. The remnant pump power at the output was measured to be $\sim 0.38\%$ of the input pump power. The slope efficiencies for the red, green and blue are 4.4×10^{-6} , 4.2×10^{-6} and 6.6×10^{-6} , respectively, with a resulting total conversion efficiency of 16.5×10^{-6} . It can be seen that, despite the fact that a single pump source is used, the three emission bands are very well balanced. This indicates that the produced fiber is well suited for lighting applications.

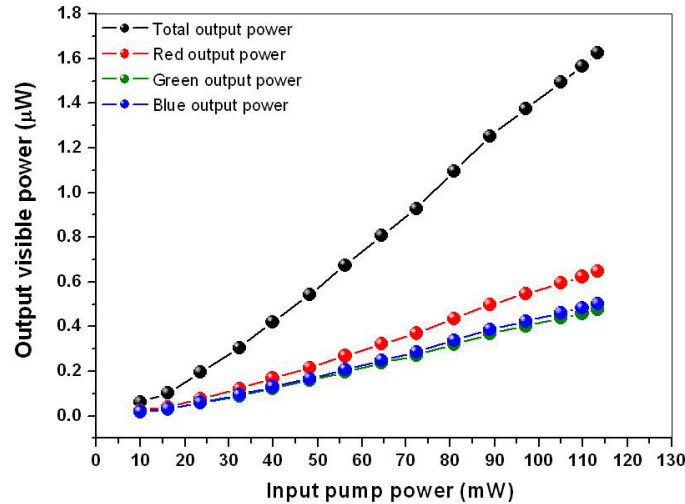


Fig. 7. Output emission power as a function of input pump power for each RGB emission and for the resulting total power.

Figure 8 shows near-field images of the emission leaving the fiber with and without band-pass filters to separate the three distinct emission bands, for a 250 mm fiber length. In particular, it is noted that without band-pass filters white light is obtained, thus, confirming the balance between bands, as shown in Fig. 7. Although the total output power varies with fiber length, the results show that the power balance between bands is kept.

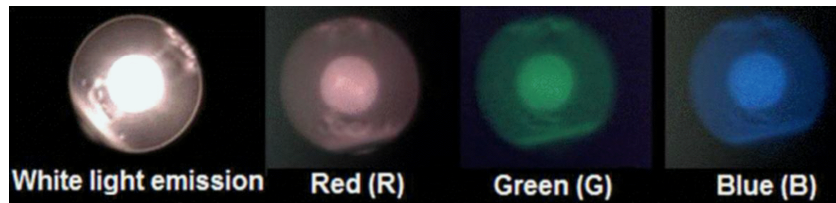


Fig. 8. Fluorescence from the end of the fiber pumped under 145 mW at 980 nm diode laser excitation. Bandpass filters were used so separate the three different emissions.

Figure 9 presents the energy level diagrams of Yb^{3+} , Tm^{3+} and Ho^{3+} ions in tellurite glass with the radiative electronic transitions corresponding to the three emission bands shown in the present work. The up conversion mechanisms involved here have been already described in the literature [21,22]: the Yb^{3+} ions absorb efficiently the 980 nm radiation and transfer the excitation energies to both Tm^{3+} and Ho^{3+} ions. On one hand, Tm^{3+} ions are excited through three successive energy transfer (ET) steps: (A) firstly, the $^3\text{F}_4$ level is excited after a non radiative relaxation from the $^3\text{H}_5$ level, (B) secondly, the second ET excites the $^3\text{F}_2$, $^3\text{F}_3$ levels from the $^3\text{F}_4$ level, and (C) after another non radiative relaxation from the $^3\text{F}_2$, $^3\text{F}_3$ levels to the $^3\text{H}_4$ one, the third ET occurs, resulting in the population of the $^1\text{G}_4$ level. The radiative relaxations corresponding to the 480 and 650 nm emission bands are the $^1\text{G}_4 \rightarrow ^3\text{H}_6$ and the $^1\text{G}_4 \rightarrow ^3\text{F}_4$ transitions, respectively. On the other hand, two successive ET from Yb^{3+} ions are

involved for the Ho^{3+} ions: the $^5\text{I}_6$ level is firstly excited from the ground state $^5\text{I}_8$ and the second ET populates the $^5\text{F}_4$, $^5\text{S}_2$ levels from the excited $^5\text{I}_6$ state (ESA). The $^5\text{F}_5$ level can be populated by two mechanisms: (i) from a non radiative relaxation from the $^5\text{F}_4$, $^5\text{S}_2$ excited states and/or (ii) from the excitation of the $^5\text{I}_7$ level from the $^5\text{I}_6$ level, itself excited after a non radiative relaxation of the $^5\text{I}_6$ state. The radiative relaxations corresponding to the 545 and 660 nm emission bands are the $^5\text{F}_4$, $^5\text{S}_2 \rightarrow ^5\text{I}_8$ and the $^5\text{F}_5 \rightarrow ^5\text{I}_8$ transitions, respectively, as depicted in Fig. 9.

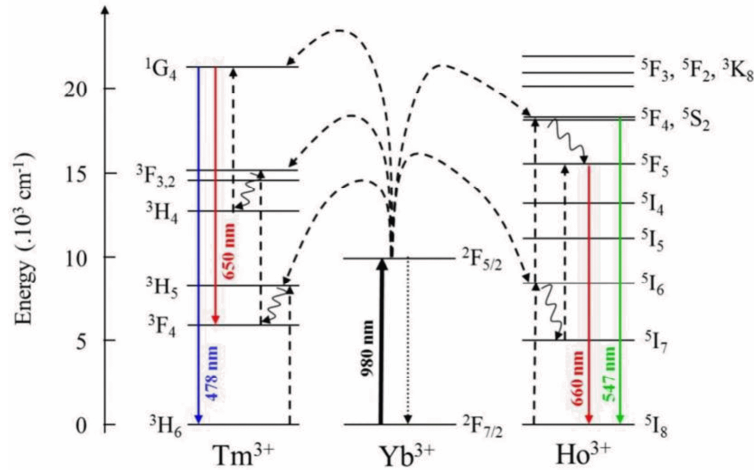


Fig. 9. Energy level diagram of Yb^{3+} , Tm^{3+} and Ho^{3+} ions with the proposed up conversion mechanisms upon 980 nm laser excitation [19].

In previous work [19] with 2 mm thick bulk samples of the same triply doped glass, some of us demonstrated that the output emission intensity in each band held a power law dependence on the input pump power that could directly be related to the number of photons involved in the respective up conversion processes (i.e. two and three photon absorption processes yielded quadratic and cubic power dependencies, respectively). In the present case, although the same transitions are believed to be present, the power-law exponents extracted from Fig. 7 are 7 for the blue emission and 5 for the red and green emissions. This is attributed to reabsorption of emitted photons along the fiber, as well as to linear losses, which cannot be neglected in the waveguide geometry. Also, absorption of emitted photons followed by re-emission (not necessarily in the same band) can also alter the power law dependence.

The CIE (Commission Internationale d'Eclairage) standard chromaticity diagram 1931 is a widely employed tool to characterize lighting materials, allowing to give account for the overall emission as perceived by the human eye. The chromaticity diagram coordinates (x , y) are calculated from the multicolor emission spectrum of the material in the visible range (from 380 to 750 nm). The (x , y) coordinates of the optical fiber emission have been, thus, calculated and plotted in the chromaticity diagram 1931, as illustrated in Fig. 10. One can observe on this diagram that the locations of optical fiber emission do not significantly change from a pump power of 48mW to 145mW, but that some tunability is possible.

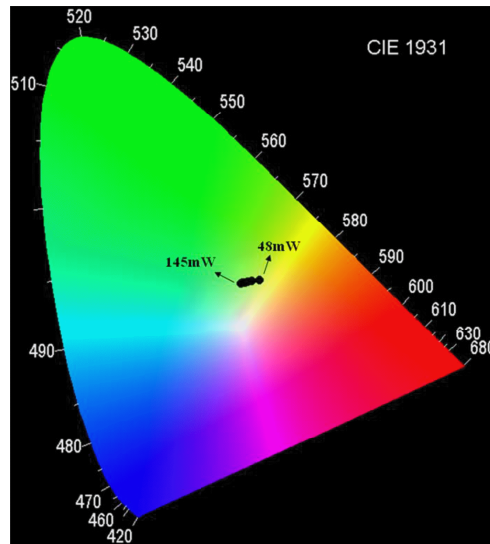


Fig. 10. CIE (x,y) chromaticity diagram showing the color coordinates of the multicolor up conversion emission of the triply-doped core optical fiber and the color tunability.

4. Conclusion

In this paper, we report a method to produce core-cladding preform, with multimode step index profile, based on $\text{TeO}_2\text{-GeO}_2\text{-Bi}_2\text{O}_3\text{-K}_2\text{O}$ and $\text{TeO}_2\text{-GeO}_2\text{-Bi}_2\text{O}_3\text{-K}_2\text{O}:(1.6\text{Yb}^{3+}/0.6\text{Tm}^{3+}/0.1\text{Ho}^{3+})$ compositions for cladding and core respectively, using the called “sucking method”. The method was effective to obtain preform with good core centricity, without bubbles and cracks, and good core-cladding interface, measured using the Tm^{3+} fluorescence at 800 nm when excited at 633 nm. This region was mapped support with a Micro-Raman equipment and was estimated for about 45 μm . The small interface approves the efficiency of the method to produce preform with respect to contamination of the cladding composition with the ions contained in the core, during the method procedure. Furthermore, this work have evidenced that the relative intensities of the RGB emission can be tuned by varying the pumping power at 980 nm. The chromaticity diagram also showing the multicolor up conversion emission of the triply-doped core optical fiber and the color tunability. A warm white color is thus produced when higher excitation laser powers are used. Such result, i.e. color tunability with the use of a single near infrared pump source, is promising in view of achieving photonic devices for solid-state three dimensional, multicolor (RGB) displays, for solid-state lighting, biomedical diagnosis.

Acknowledgments

The authors acknowledge CNPq and Instituto Nacional de Fotônica – InFo, for financial support. We also acknowledge Dr. Jefferson L. Ferrari for his scientific contribution.